

ON-ORBIT STELLAR CAMERA CALIBRATION BASED ON SPACE RESECTION WITH MULTI-IMAGES

Xie Junfeng^a, Jiang Wanshou^{a*}, Gong Jianya^{a*}, Wang xiao^a

^a State Key Laboratory of Information Engineering in Surveying, Mapping and Remote Sensing, Wuhan University, Luoyu Road 129, Wuhan, China, 430079 -junfengxie@gmail.com (jws, jgong)@lmars.whu.edu.cn wclearwaters@gmail.com

KEY WORDS: on-orbit calibration, stellar camera, space resection, multi star images, satellite attitude accuracy

ABSTRACT:

Due to the intense vibration and/or the change of space environmental factors such as temperature, pressure, etc., the stellar camera parameters might change during satellites launching or while orbiting the earth, which causes the decline of satellite attitude accuracy. So the on-orbit calibration is essential for the stellar camera. In this paper, the selection of star image for on-orbit calibration is discussed. From experiment, it can be concluded that for the on-orbit calibration based on space resection, the distribution of star image points has strong effect on the calibration accuracy, and a good selection of images can significantly improve the calibration accuracy.

1. INTRODUCTION

Satellite attitude determination is not only the basis of satellite attitude control, but also one of the effective means to improve the direct location accuracy of remote sensed imagery (spot image, 2005). At present, attitude determined by star sensor is one of main satellite attitude determination methods (Levine et al., 1991; Jorgensen and Pickles, 1998; Eisenma and Liebe, 1997).

There are many factors affecting the accuracy of satellite attitude determined by star sensor, and the calibration accuracy of the stellar camera parameters is an important factor (Xie, 2007). Although the stellar cameras parameters have been calibrated on the ground before the satellite launches, the camera parameters might change when the satellite had intense vibration in the process of launching and/or the space environmental elements such as temperature, pressure, etc. have changes. All of them will cause the decline of the stellar camera parameters accuracy directly. Therefore, the on-orbit calibration for stellar camera is very essential to assure the attitude accuracy.

So far, there are a few on-orbit calibration methods for the stellar camera. US Texas T&M University Ju and Samaan proposed a calibration method to calibrate the interior orientation elements of the stellar camera, which uses the equation of the sine or cosine of two angle distances. One angle distance is denoted by two star image points in one image, and another is described by the right ascension and the declination of two corresponding guide stars (Ju, 2001; Samaan, 2003). Chen had researched a on-orbit calibration method for star sensor with gyro (Chen and Geng, 2006). Wang puts forward a stellar calibration method for the ground camera on the ground. This method directly considers the stars as the control points, and calibrates the camera parameters based on space resection (wang, 1979). This approach is adopted for on-orbit measurement of the stellar camera parameters in this paper.

In this approach, because the Field Of View (FOV) of the stellar camera is narrow, the number and distribution of stars in one single image acquired at each moment is not necessarily beneficial for the stellar camera calibration. When the satellite orbits the earth, a large number of stellar images can be obtained by the stellar camera in a short time, and the environment factors has little effect on the stellar cameras within this time, so the camera parameters can be considered unchanged, then multi images can be accumulated to improve the quality of control points. At present, dozens of even hundreds of star images acquired within a few minutes have been used to calibrate the stellar camera (JU, 2001). But it doesn't take into account whether the distribution of stars affect the calibration result, and it generally uses all identified star images directly, but the more number of star images doesn't necessarily mean the higher calibration accuracy. Moreover, it may take long time for calibration. Therefore, selection of Image in view of the distribution is a problem needed be considered in this approach.

2. ON-ORBIT CALIBRATION BASED ON THE SPACE RESECTION

2.1 The principle of the on-orbit calibration

On-orbit calibration for stellar camera uses the star image point coordinates as observations, and error equations of unknown parameters can be established based on the collinearity equation. The unknown parameters include the attitude angles and the stellar camera parameters. The camera parameters contain the principal point offset (x_0 , y_0) and the focal length (f), the optical distortion of the CCD, mainly including the radial distortion and the tangential distortion, etc.. The radial distortion coefficients are denoted by K_1 , K_2 . Since the tangential distortion of CCD has little impact on attitude accuracy, it isn't considered in this paper.

The camera parameters before calibration are thought as initial values. Likewise, the attitude angles solved based on the collinearity equation with the initial camera parameters are

thought as initial attitude angles. The more precise camera parameters are obtained by iterative process based on the least square technique.

Different from traditional coordinate systems in photogrammetry, the attitude angles in the celestial sphere coordinate system are shown in figure 1. α_0 , δ_0 and k denotes the attitude angles (Wang, 1979). When compared to the distance of the star to the Earth, the distance of star sensor to the Earth can be omitted, so the geocentric position is always considered be the projection centre (Xu, 1998), thus each image has only three attitude angles as exterior orientation elements.

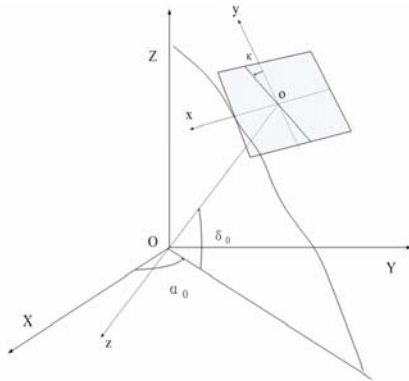


Figure 1. The attitude definition in the celestial sphere coordinate system

Rigorous collinearity equation in the celestial sphere coordinate system is shown as below:

$$\begin{cases} x-x_0+\Delta x=-f \frac{a_1 \cos \alpha \cos \delta+b_1 \sin \alpha \cos \delta+c_1 \sin \delta}{a_3 \cos \alpha \cos \delta+b_3 \sin \alpha \cos \delta+c_3 \sin \delta} \\ y-y_0+\Delta y=-f \frac{a_2 \cos \alpha \cos \delta+b_2 \sin \alpha \cos \delta+c_2 \sin \delta}{a_3 \cos \alpha \cos \delta+b_3 \sin \alpha \cos \delta+c_3 \sin \delta} \end{cases} \quad (1)$$

Where α = the right ascension of the star,
 β = the declination of the star,
 $(a_i, b_i, c_i)_{(i=1,2,3)}$ = Nine elements in the attitude rotation matrix.
 $\Delta x, \Delta y$ = the distortions of the CCD.
 $\Delta x=(x-x_0)(k_1 r^2+k_2 r^4+k_3 r^6)$,
 $\Delta y=(y-y_0)(k_1 r^2+k_2 r^4+k_3 r^6)$
 $r=\sqrt{(x-x_0)^2+(y-y_0)^2}$
 K_1, k_2, k_3 = the second-order and fourth-order and sixth-order coefficients of r in the radial distortion

For single star point, if the image point is viewed as observed value (v), and the principal point offset (x_0, y_0) and focal length (f), and the attitude angle are considered as unknowns, the error equation can be founded as follows:

$$\begin{bmatrix} V_x \\ V_y \end{bmatrix} = \begin{bmatrix} \frac{\partial x}{\partial \varphi} & \frac{\partial x}{\partial \omega} & \frac{\partial x}{\partial \kappa} & \frac{\partial x}{\partial f} & \frac{\partial x}{\partial x_0} & \frac{\partial x}{\partial y_0} \\ \frac{\partial y}{\partial \varphi} & \frac{\partial y}{\partial \omega} & \frac{\partial y}{\partial \kappa} & \frac{\partial y}{\partial f} & \frac{\partial y}{\partial x_0} & \frac{\partial y}{\partial y_0} \end{bmatrix} \begin{bmatrix} \Delta \varphi \\ \Delta \omega \\ \Delta \kappa \\ \Delta f \\ \Delta x_0 \\ \Delta y_0 \end{bmatrix} - \begin{bmatrix} x-(x) \\ y-(y) \end{bmatrix} \quad (2)$$

The differential coefficient of equation (2) can be derived. 2n error equations can be given if there are n points. The optimal unknowns are obtained by iterative process based on the least square technique. The process is stopped when the correction of unknown parameters are less than the predefined thresholds.

2.2 Experiment procedure

The experiment procedures are shown as figure 2. The real star catalogue is adopted in this experiment to provide the right ascension and declination of the guide stars. Suppose the camera parameters before calibration and the real camera parameters are known, the star image coordinates can be simulated based on the imaging principle when the real attitude angles are set. Initial attitude angles are computed with these simulated star images coordinates and the camera parameters before calibration, which are considered as initial attitude angles. The more accurate camera parameters and attitude angles can be obtained based on space resection with initial camera parameters and attitude angles. The difference value of the calibrated camera parameters and the real camera parameters can be thought as the standard to evaluate the calibration accuracy.

During the simulated process, the random position error within 0.1-0.5 pixel is added into image points individually. At present, the extraction accuracy of the star image points has achieved 0.1 pixel (Quine et al., 2007), so the simulation is reliable.

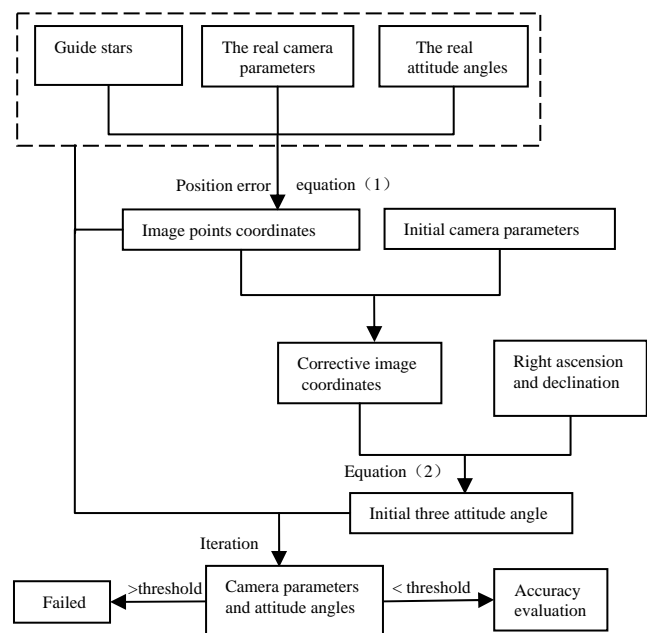


Figure 2. Experiments procedure of on-orbit calibration

3. STAR IMAGE SELECTION

As related above, this on-calibration method is based on star images. But not all star images are identified successfully by the reasons of the asymmetry distribution of stars in the celestial sphere, or the insufficiency of the number of the detected stars, or the limitation of the star identification algorithm etc. (Liebe, 1995). Only the identified star images can reach the basic requirement for calibration, in other words, the number of star image points of each calibrated image is more than three at least.

In this foundation, the distribution of star image points of each calibrated images should be considered, because the calibration accuracy has correlation with the distribution of control points (Feng, 2002). Ten sequential images in one calibration period are shown in the figure 3. It is seen from it that different image has different distribution, and the calibration accuracy based on different image may be different.

In this paper, the convex area method is used to evaluate whether this image is eligible for calibration. Take the eighth star image as an example, which is shown in figure 4. The steps of this method are as follow:

- (1) The convex is constructed by the star image points on the edge of the image by the convex algorithm (Jin et al., 1999; Zhou et al., 2003; Rourke, 1998).
- (2) As the coordinates of connection point is known, so then the area of the convex is computed.
- (3) The area percent of the convex in the whole image is got. If the percent is more than fifty percent, which indicates the distribution is relatively even, the distribution of the image is considered good and the image is selected.

From figure 3, the result evaluated by the convex area method is the distribution of figures (e), (g), (h), (j) are good and figures (b), (c), (d) are bad.

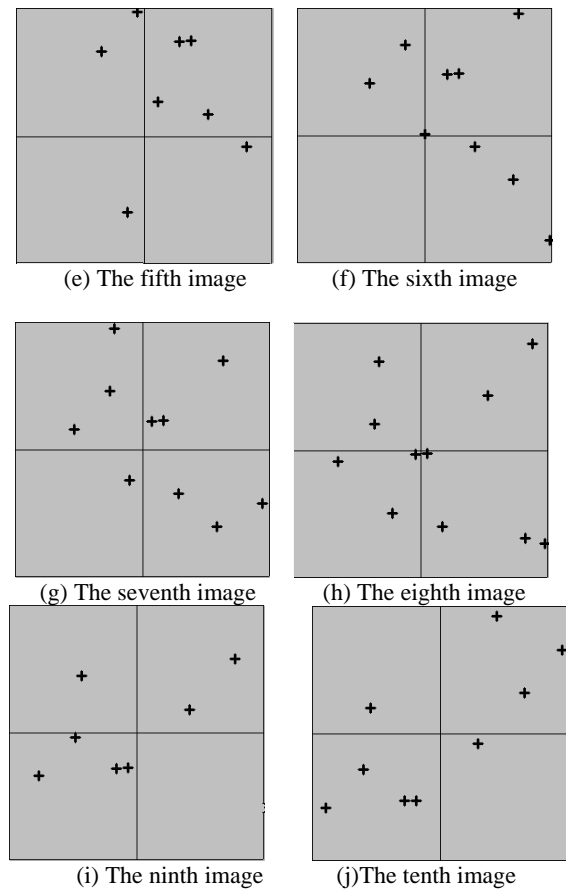
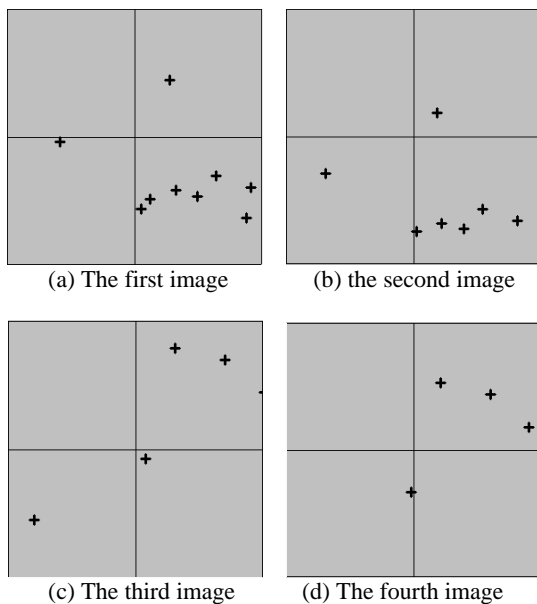


Figure 3. The distribution of part of images

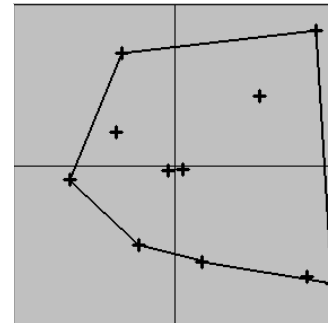


Figure 4. Convex constructed by star image points

4. EXPERIMENT

The star catalogue Tycho-2 (J2000)(Li, 2006) was downloaded for experiment, whose data types include star index, magnitude, the right ascension (hour, minute, second) and the declination (degree, arcminute, arcsecond) etc.. Average positions of the stars in standard epoch are transformed to intraday visual position in real attitude determination. The FOV is $8^{\circ} \times 8^{\circ}$, and the size of array CCD is 512×512 pixels, and each pixel size is 13 μm . The upper and lower limit of magnitude is 0 and 6.0 (mv), and then there are 5001 stars selected in star catalogue for these experiments. Supposed one stellar image is got by the stellar camera each 0.1 second, and the calibration period is 2 second in this experiment in the experiments.

The real on-orbit camera parameters are set as follow, $\hat{f}_0 = 3660.97(p)$, $\hat{x}_0 = 35(p)$, $\hat{y}_0 = 35(p)$, $\hat{k}_1 = 3e-8(p^{-2})$, $\hat{k}_2 = 1e-13(p^{-4})$, (Note: p denotes pixel, and the below is the same). The camera parameters before calibration are given as below, $f_0 = 3655.97(p)$, $x_0 = 0(p)$, $y_0 = 0(p)$, $k_1 = 0(p^{-2})$, $k_2 = 0(p^{-4})$.

4.1 The calibration experiment based on the single image and multi-images

After the real camera parameters and the attitude angles are given, the star image point coordinates can be simulated, then each image point is added with the position error 0.1 pixel. Ten continuous images in the one calibration period are selected. First, the calibration is done using each star image data independently, then the process is repeated using all ten images, the calibration results are shown in table 1. (Note: the calibration accuracy is denoted by absolute difference value of the calibrated parameter values and the real parameter values).

Camera Parameters accuracy	Δf (p)	Δx_0 (p)	Δy_0 (p)	Δk_1 (P^{-2}) (10^{-9})	Δk_2 (P^{-4}) (10^{-14})	
Single image	1	2.01	8.75	11.25	23.51	20.45
	2	9.77	4.50	7.63	77.57	49.30
	3	18.15	61.80	37.10	130.6	70.93
	4	16.84	300.3	207.4	21.01	19.99
	5	0.7	1.70	1.04	6.23	4.92
	6	1.26	11.90	6.99	19.11	8.89
	7	0.16	6.44	0.72	15.91	25.67
	8	2.55	0.37	5.13	13.78	8.85
	9	2.00	42.87	24.45	9.18	13.07
	10	0.64	4.46	17.45	6.00	1.93
ten images	0.57	1.97	1.37	3.89	3.67	

Table 1. Calibration result based on single image and ten images separately

It can be seen from table 1, of all the calibration results based on each single image, only these using the fifth, seventh, eighth and tenth image are relatively good, although the accuracy isn't high. The calibration results based on the other images are worse. As seen from figure 3, the good calibration results are based on the images which have good distribution. But for most other image, the natural distribution of it is difficult to satisfy the calibration requirement, so the calibration accuracy is low

From table 1, the calibration result is based on all ten images is better than based on each single image. The reason is that there are only three unknowns for each star image, but this image can provide three control points at least to calibrate the camera parameters, when the star images which have good distribution is added for calibration, the calibration accuracy become better.

4.2 The relationship between the calibration accuracy and the number of images

Suppose that the camera parameters before and after calibration are same with experiment above, when the random position

error 0.1 pixel is added in the image coordinates, the calibration experiments are done with 1-10 images separately, the relationships between the number of the images and the principle distance, the principle points and the distortion coefficients are shown in figure 5,6,7,8.

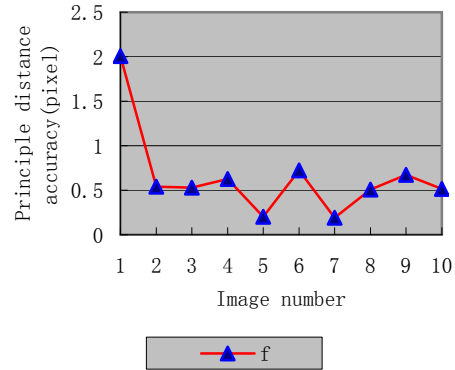


Figure 5. The relationship between the principle distance and the number of images

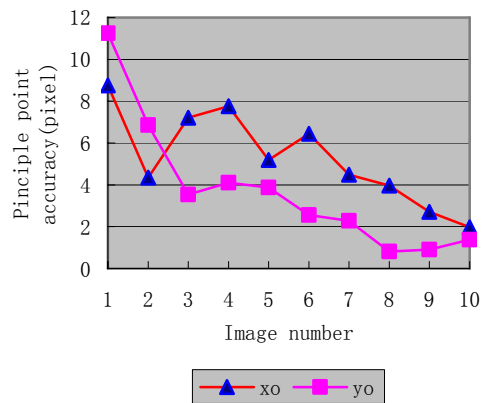


Figure 6. The relationship between the principle point and the number of images

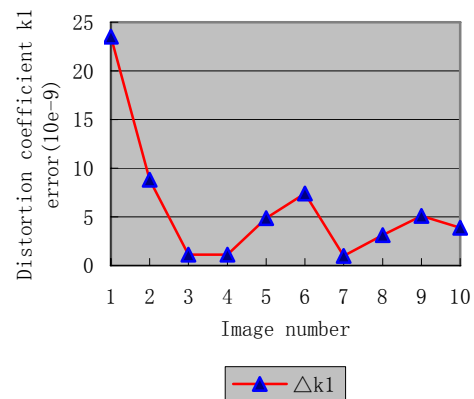


Figure 7. The relationship between the distortion coefficient k1 and the number of images

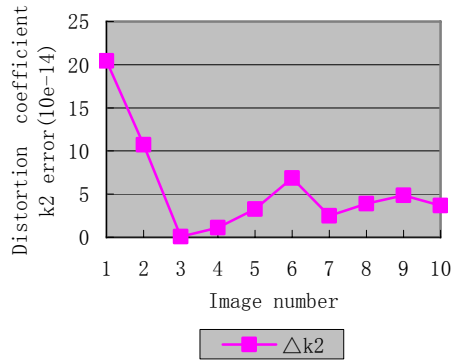


Figure 8. The relationship between the distortion coefficient k_2 and the number of images

As can be seen from figures 5,6,7,8 with the incensement of number of images, there are an overall improvement trend in the calibration accuracy of the camera parameters, but the tendency isn't consistent. The reason is that the distribution of all participated images will affect the calibration result during the calibration process. Generally, when the number of participated images increases, the probability of the calibration with high accuracy becomes larger, but if the distribution of the control points in the later joined image is bad, the whole calibration accuracy will drop.

4.3 Calibration Experiment based on selected multi images

Based on the analysis above, the more the number of images doesn't mean the higher the calibration accuracy, which depends on the distribution of each participated image. Based on the distribution of each star image, the fifth, the eighth, and the tenth images are selected as the first set images, and the calibration result based on these three images is noted by C3. In the same way, the fifth, the seventh, the eighth and the tenth images are selected as the second set images, and the calibration result is denoted by C4. The first, the fifth, the seventh, the eighth and the tenth images are selected as the third set images, and the result is denoted by C5. Lastly, the calibration result using the all ten images is noted by C10. All the calibration results are shown in Figure 9.

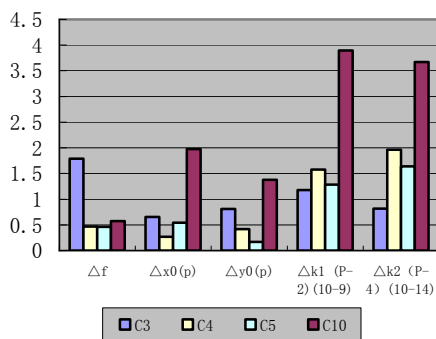


Figure 9. The comparison based on selected combine images and all images

It is seen that the calibration accuracy based on the selected images are better than based on all ten images, which indicates that the calibration result based on all images isn't necessarily

highest. Meanwhile, it verifies that selecting image in view of the distribution of participated image is very important step to improve the on-orbit calibration accuracy of the stellar camera.

5. CONCLUSION

During the attitude determination by star sensor, the change of the stellar camera parameters might cause the decline of the attitude accuracy, the on-orbit calibration method based on space resection is employed. Selecting image for this approach is proposed in this paper.

From experiment, two conclusions are drawn. For the on-orbit calibration based on space resection, the distribution of star image points has strong effect on the calibration accuracy, and a good selection of images can significantly improve the calibration accuracy.

Therefore, automatically selecting the star images considering its distribution is essential for this approach, which has the practical meaning for improving the calibration accuracy and accelerates the on-calibration period.

REFERENCE

Chen, X., and Geng, Y., 2006. On-orbit calibration algorithm for gyros/star sensor. *Journal of Harbin Institute of Technology*, 38(8), pp.1369-1373.

Eisenma, A.R., and Liebe, C.C., 1997. The new generation of autonomous star trackers. *SPIE*, Vol. 3221, pp.524-535.

Feng, W., 2002. *Close-range Photogrammetry (in Chinese)*. Wuhan University Press, pp.187-193

Jin, W., and He, T., and Tang, W., 1999. Simple fast convex hull algorithm of planar point set. *Journal of Beijing University of Aeronautics and Astronautics*, 25 (1), pp.72-75.

Ju, G., 2001. Autonomous star sensing, pattern identification and attitude determination for spacecraft: An analytical and experimental study (PhD), Texas A&M University, pp.176-177

Liebe, C.C., 1995. Star trackers for attitude Determination. *IEEE AES Systems Magazine*, pp.10-11.

Li, Z., 2006. Star catalogue. <http://lzk.lamost.org/>

Levine, S., Dennis, R., and Bachman, K.L., 1991. Strap down astro-inertial navigation utilizing the optical wide-angle lens star tracker, Navigation. *Journal of the Institute of Navigation*, 37(4), pp.347-362.

Quine, B.M., Tarasyuk, V., Mebrahtu, H., and Hornsey, R., 2007. Determining star-image location: A new sub-pixel interpolation technique to process image centroids computer physics communications, pp.1-7.

Rourke, J.O., 1998. *Computational Geometry in C, 2nd Ed.* Cambridge University Press, Cambridge, UK.

Samaan, M.A., 2003. Toward faster and more accurate star sensors using recursive centroiding and star identification (PhD), Texas A&M University, pp.25-29.

Spot image, 2005. Pre-processing levels and location accuracy ,Technical information. www.spotimage.com

Wang, Z., 1979. *Principles of Photogrammetry with remote sensing*. Publishing House of Surveying and Mapping, pp.167-169

Xie, J., and Jiang, W., 2006. *The analysis of the error sources affecting the accuracy of Attitude determined by star sensor*, *The 15th International Conference on Geoinformatics*, Nan Jing,China Vol. 6752,Part 2, PP.675248-2-675249-8.

Xu, S., 1998. Coordinate Transformation in Real-Time Star Field Simulator. *Journal of Harbin Institute of Technology*, 30(5), pp. 118-120.

Zhou, P., Liu, J., and Wang, L., 2003 An algorithm for finding a convex hull of the vertices of a polygonal line. *Journal of Beijing Institute of Technology*. 23 (1) ,pp.75-77.

ACKNOWLEDGEMENTS

This work was supported by the National Basic Research Program of China under Grant 2006CB701300-G.